ACCSCIENCE PUBLISHING

International Journal of Bioprinting

RESEARCH ARTICLE

A parallel multilayered neurovascular unit-on-a-chip for modeling neurovascular microenvironment and screening chemotherapeutic drugs

Supplementary File

1. Supplementary methods

1.1. Quantitative real-time polymerase chain reaction (qRT-PCR)

To compare the relative gene expression levels between the groups, total RNA was collected from each sample (n = 3, technical repeats = 3 per group) using the RNeasy Mini kit (TIANGEN, Beijing, China), and complementary deoxyribonucleic acid (cDNA) was synthesized using the cDNA synthesis kit (TIANGEN, Beijing, China) according to the manufacturer's instructions. The samples in this experiment are all the cells on the hNVU chip device. The cell extraction steps are described below: (1) Extraction of hCMEC/D3 cells from the BBB: 0.25% trypsin was used to digest the hCMEC/D3 cells on the PET membrane, the enzymatic hydrolysis was stopped, and the cells were pelleted and collected by centrifugation. TRIpure Reagent (1 mL) was added and pipetted repeatedly to lyse the cells. The extraction method can be found in the manufacturer's instructions of the reagent. (2) Extraction of cells in the brain area: collagenase was added to sterile PBS solution, diluted to 0.3 mg/mL to obtain the working solution of the lysate, and set aside. Sterile scalpels, tweezers, scissors, etc. were used. The sample was cut and transferred into a 15 mL sterile centrifuge tube prior to being shredded. The lysis working solution was added, and the centrifuge tube was placed in a 37°C water bath and shaken. Lysis was observed every 1 min. After full lysis was achieved, precooled centrifugation was performed at 1000 rpm for 5 min, the supernatant was discarded, precooled PBS was added, and washing and centrifugation were repeated 1 or 2 times. TRNzol extract was added to save the collected cells (clusters) for further PCR experiments. Subsequently, the RNA reverse-transcription kit containing DNase (PrimeScript RT Master Mix kit, Takara, Japan) was used at 42°C to remove the contamination of genomic DNA, and 2 μg of RNA was reverse-transcribed into cDNA. Gene expression level analysis was then performed using a qPCR kit (SYBR Premix Ex Taq kit, Takara, Japan) and a QuantStudio 6 qPCR instrument (Thermo, USA). The expression level of each target gene was normalized to that of the endogenous reference GAPDH. The relative gene expression levels were determined using the comparative $2^{-\triangle\triangle Ct}$ method. The primers used in this study are listed in Table S2.

1.2. Detection of chemotherapeutic drug concentration

AB SCIEX QTRAP analysis™ 4500 (United States) triple quadrupole mass spectrometer was used, which contained SRM-positive or -negative ionization mode. On the ACQUITY UPLC HSS T3 analysis column (2.1 × 50 mm, 1.8 μm), ACQUITY UPLC I-Class (Waters, USA) infinite binary pump was used. LC separation was performed on water. Gradient elution was performed using acetonitrile/methanol (1:1, v/v) as solvent A. Formic acid (0.1%) in water was used as elute solvent at a flow rate of 0.2 mL/min. The initial condition was for 80% solvent B to decrease to 0% solvent B within 2 min and maintain for 2 min. At 4.1 min, the initial ratio was restored and balanced for 3 min to end the analysis. The column temperature was maintained at 40°C, the sample was maintained at 10°C, and the injection volume was 5 μL. The MS parameters are as follows: ESI ion source temperature is 500°C; curtain gas: 30 pounds per square inch; collision activation dissociation (CAD) gas settings: medium; ion implantation voltage: 5500 V/-4500 V; ion gas: 1:50 pounds per square inch. Vorinostat was identified as m/z 265.2, and the confirmed ions were m/z 232.1 (quantitative ions) and 172.2. The cluster removal voltage was 70 V, the collision energy was 14 eV, and the retention time was 2.02 min. 5-fluorouracil (5-FU) was identified as m/z 129, and the confirmed ion was m/z 42 (quantitative ion). The voltage for de-clustering was -50 V, the collision energy was -22 eV, and the retention time was 1.68 min. Compound analysis on all data was performed using Analyst Software 1.6.4 software.

The standard curves of 5-FU and vorinostat concentration detected and analyzed by HPLC are shown in Figures S20 and S21, respectively.

1.3. Labeled metabolites of isotopomers measurement by GC–MS

Nonsugar metabolites were derivatized for GC/MS analysis following a previously published protocol. Cells were ground in liquid nitrogen, resuspended in 0.6 mL of cold (-40°C) 50% aqueous methanol containing 100 μM norvaline as an internal standard, and placed on dry ice for 30 min. Then, the samples were thawed on ice. Next, 0.4 mL chloroform was added and vortexed for 30 s before centrifugation for 15 min at 14,000 rpm (4°C), and the supernatant was transferred to new 1.5 mL tubes to evaporate and stored at -80°C before analysis. Metabolites were derivatized for GC/MS analysis as follows: First, 70 μL of pyridine was added to the dried pellet and incubated for 20 min at 85°C. After cooling, 30 μL of N-tert-butyldimethylsilyl-N-methyltrifluoroacetamide (Sigma) was added, and the samples were reincubated for 60 min at 85°C before centrifugation for 15 min at 14,000 rpm (4°C). The supernatant was transferred to an autosampler vial for GC/MS analysis. A Shimadzu QP-2010 Ultra GC-MS was programmed with an injection temperature of 250°C and injected with 1 μL of sample. The GC oven temperature started at 110°C for 4 min, increased to 230°C at 3°C/min and to 280°C at 20°C/min with a final hold at this temperature for 2 min. The GC flow rate with helium carrier gas was 50 cm/s. The GC column used was a 20 m × 0.25 mm × 0.25 mm Rxi-5ms. The GC–MS interface temperature was 300°C, and the (electron impact) ion source temperature was set at 200°C, with a 70 V ionization voltage. The mass spectrometer was set to scan an m/z range of 50–800 with a 1 kV detector.

GC/MS data were analyzed to determine isotope labeling and quantities of metabolites. Metabolites with baseline separated peaks were quantified on the basis of total ion count peak area using standard curves generated from running standards in the same batch of samples. To determine 13C labeling, the mass distribution for known fragments of metabolites was extracted from the appropriate chromatographic peak. These fragments contained either the whole carbon skeleton of the metabolite, which lacks the alpha carboxyl carbon, or (for some amino acids) contained only the backbone minus the side chain. For each fragment, the retrieved data comprised mass intensities for the lightest isotopomer (without any heavy isotopes, M0) and isotopomers with increasing unit mass (up to M6) relative to M0. These mass distributions were normalized by dividing by the sum of M0 to M6 and corrected for the natural abundance of heavy isotopes of the elements H, N, O, Si, and C using matrix-based probabilistic methods as described and implemented in MATLAB. Labeling results are expressed as the average fraction of the particular compound that contains an isotopic label from the particular precursor.

2. Supplementary figures

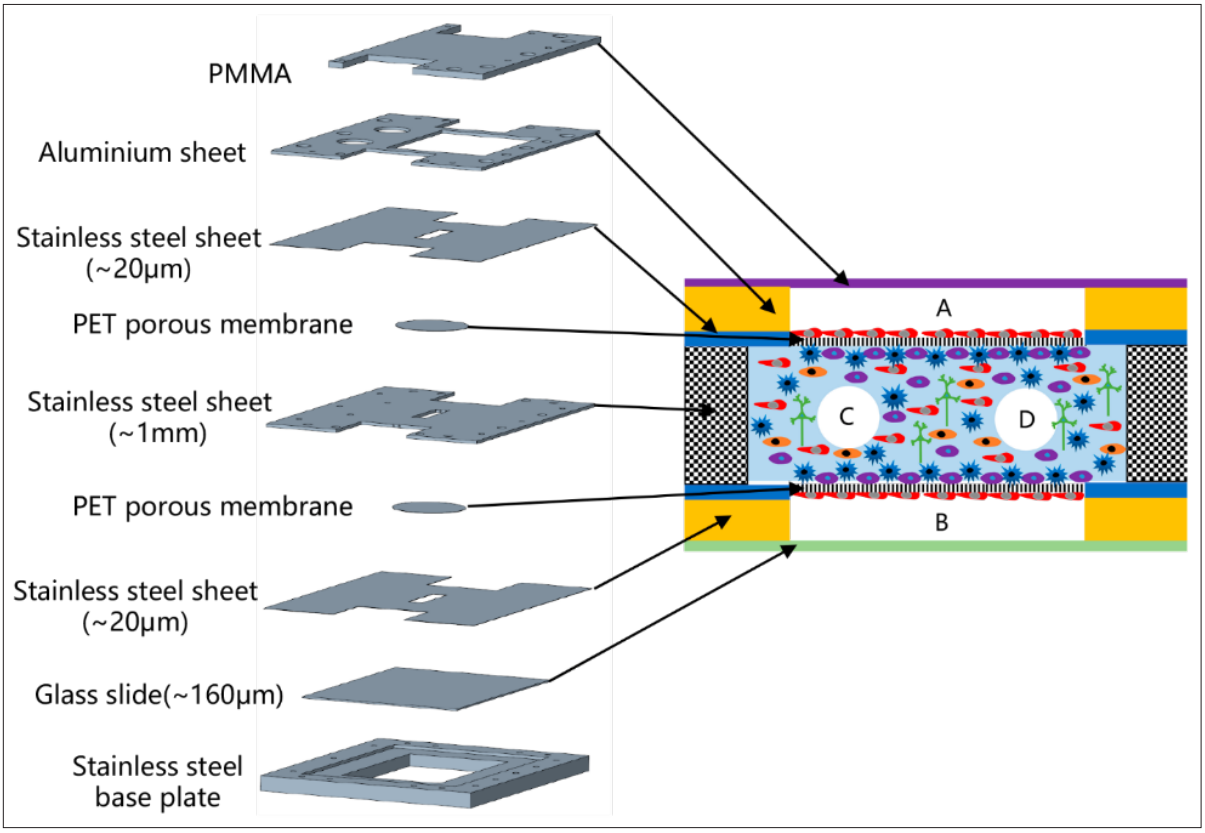

Figure S1. Schematic diagram and exploded view of the hNVU chip.

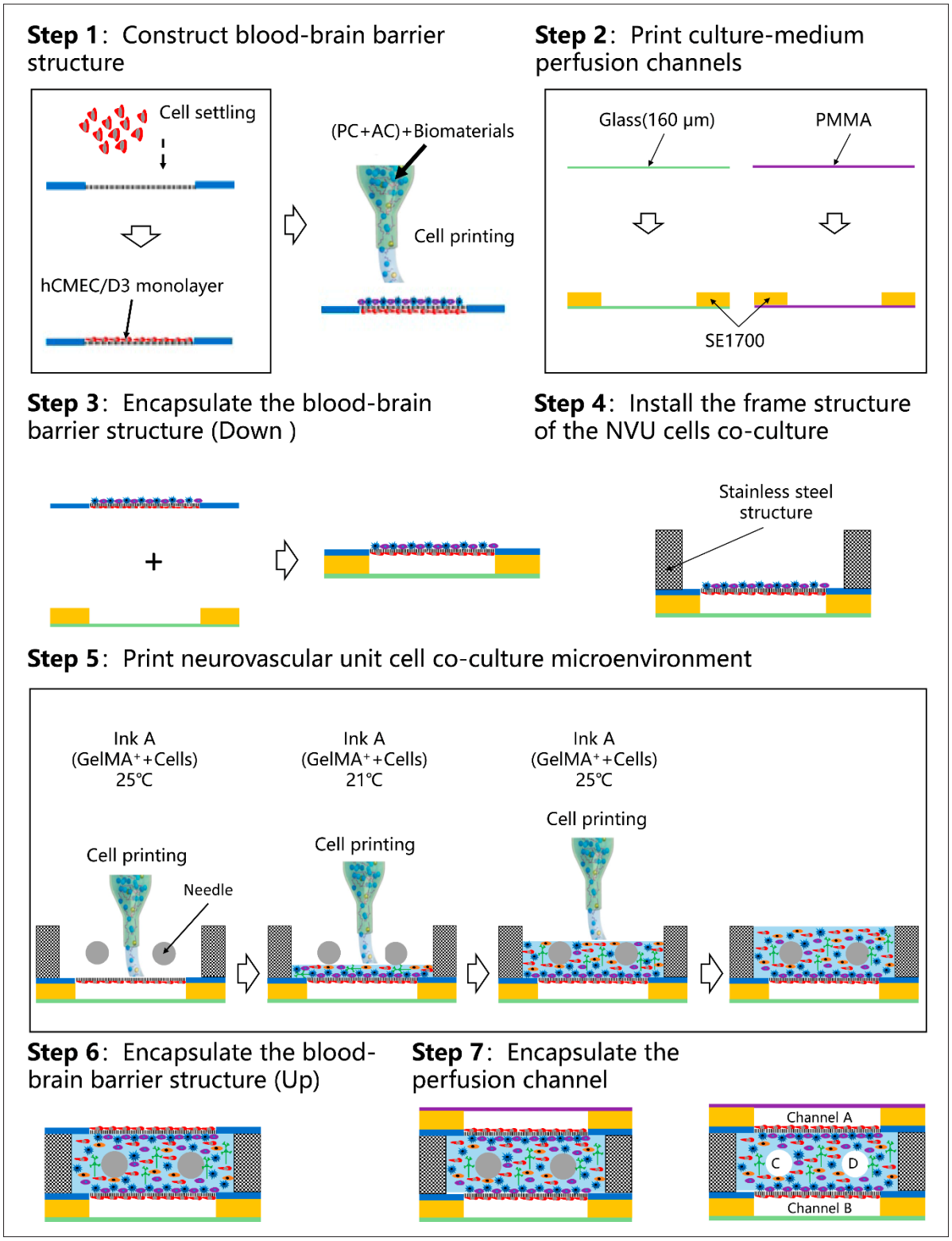

Figure S2. Fabrication step of the hNVU chip system.

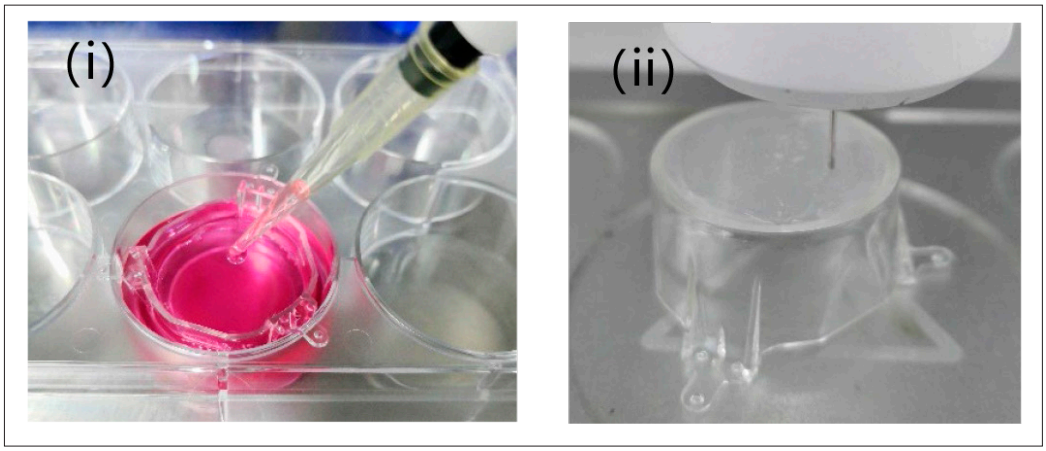

Figure S3. Fabrication of the BTB structure for the hNVU chip.

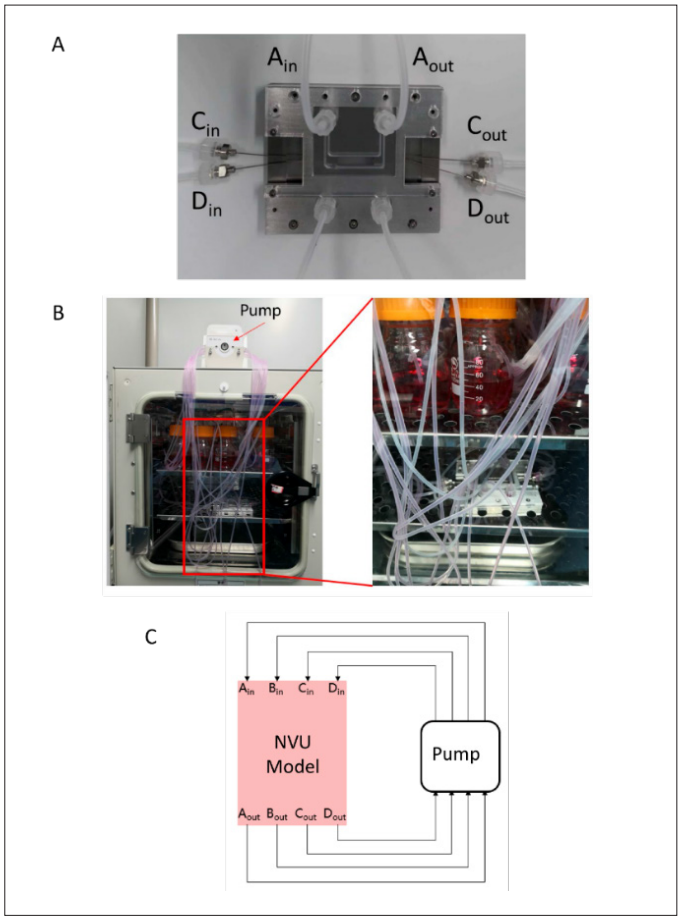

Figure S4. (A) Photograph of the hNVU chip. (B) Perfusion system for the hNVU chip. (C) Schematic diagram of the interface connection of each channel (channel A, B, C, D).

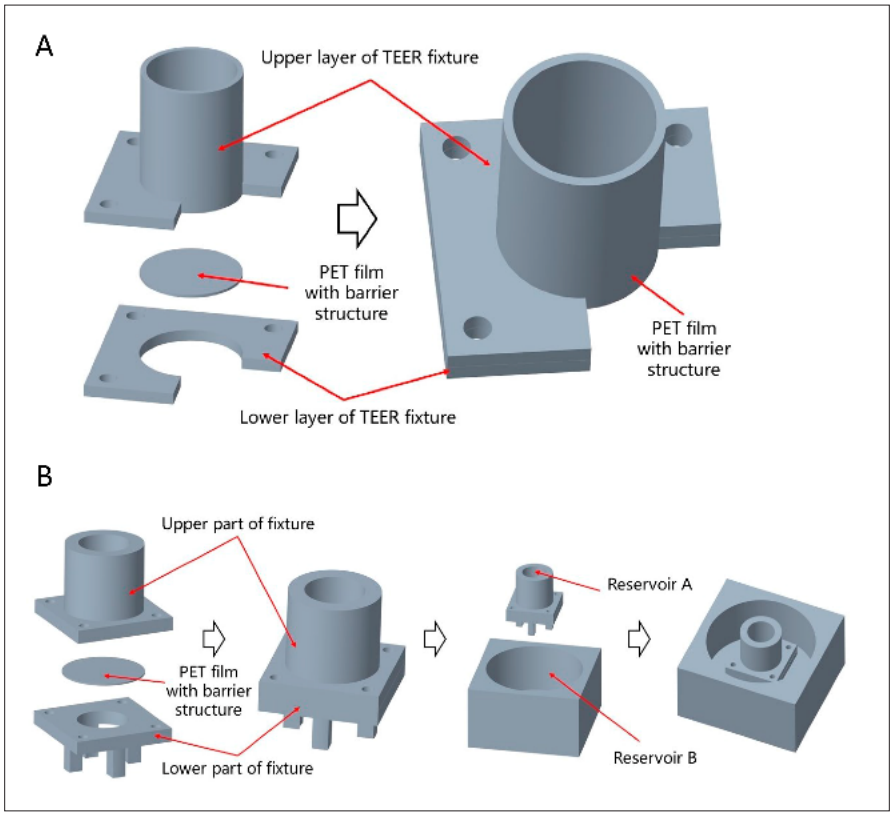

Figure S5. (A) Homemade jig for TEER measurement. (B) Custom device for measurement of barrier permeability.

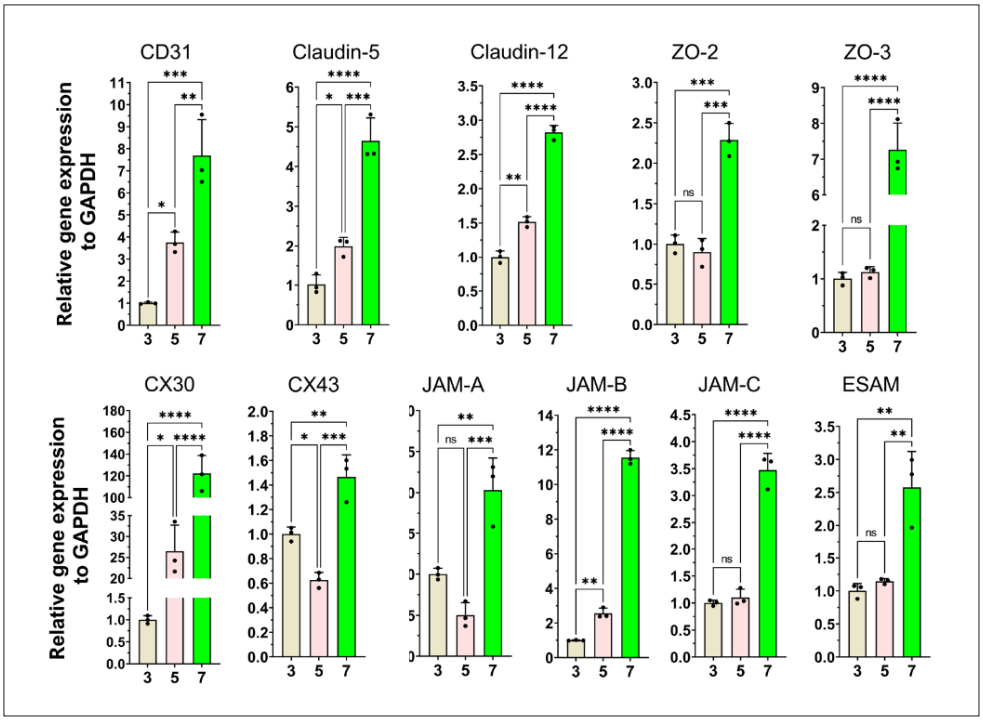

Figure S6. qRT-PCR analysis of genes associated with BTB integrity. $n = 3$, independent experiments. Data are presented as the mean ± S.D. Significant differences between the groups were determined by *t*-test.

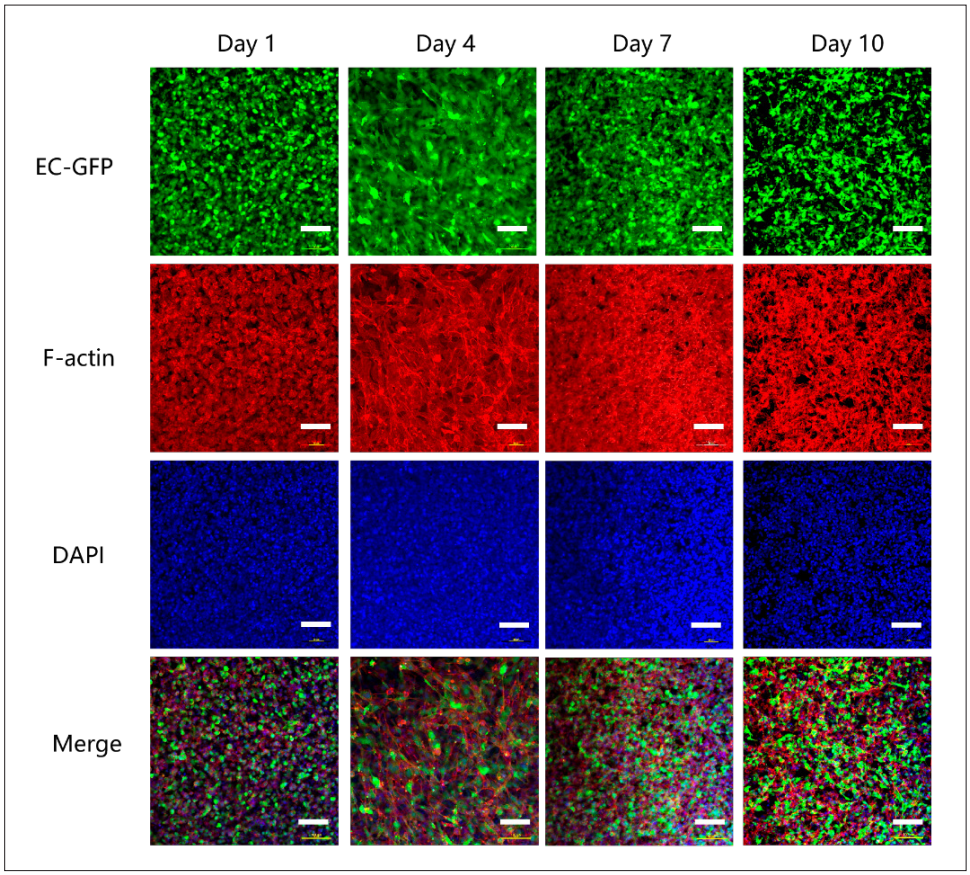

Figure S7. Morphological changes of endothelial cells in the hNVU chip. The ECM was GelMA$^+$ (5% GelMA + 2.5 mg/mL fibrinogen + 5% gelatin + 20 μg/mL laminin + 3 U/mL transglutaminase). The cell ratio was 12:4:4:4:1, and the total cell density was 2.5×10^7/mL. Scale bar: 100 μm.

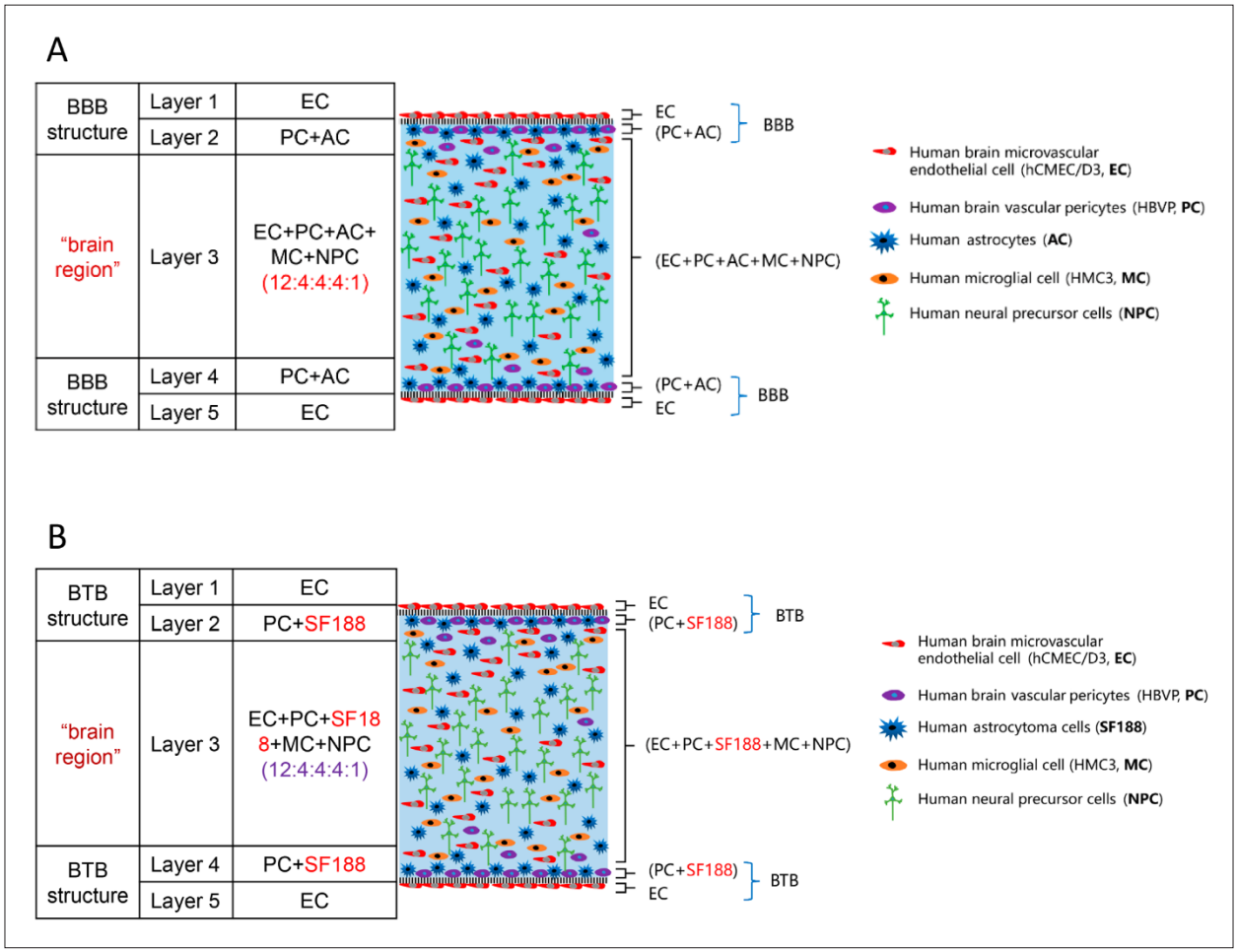

Figure S8. Hierarchically distributed hNVU model.

	(Basal medium + serum) proportional relationship					Supplement concentration percentage (relative to single cell complete medium,%)				
	E	P	A	M	N	E	P	A	M	N
G4 medium	3/7	1/7	1/7	1/7	1/7	100	100	100	100	100
G5 medium	1/8	1/8	1/8	1/8	4/8	100	100	100	100	100
G6 medium	1/5	1/5	1/5	1/5	1/5	100	100	100	100	100

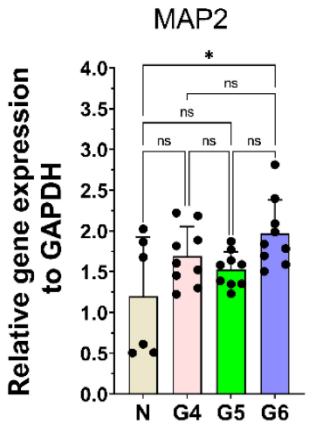

Figure S9. Effects of culture media on MAP2 gene expression at day 7.

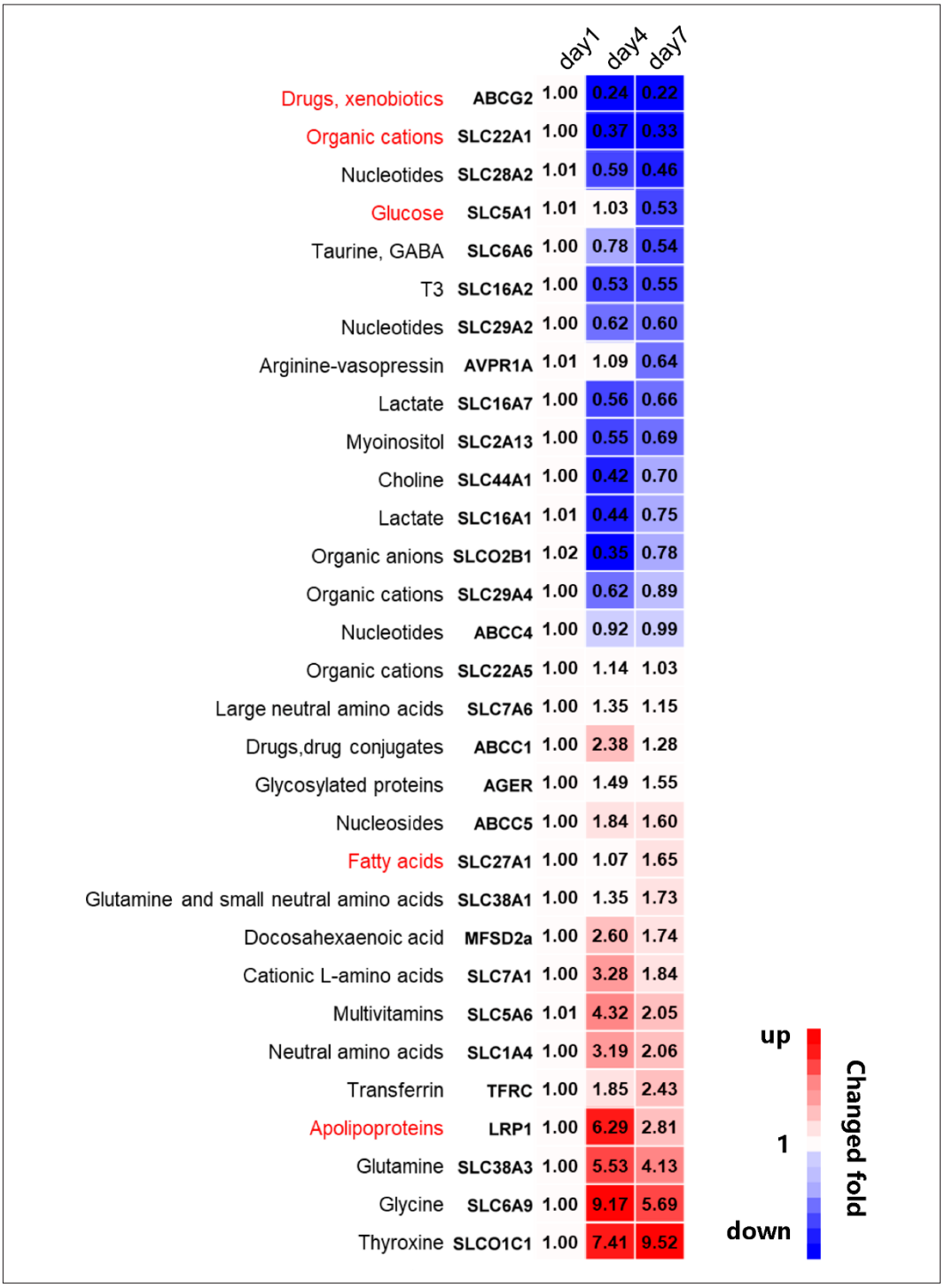

Figure S10. Molecular atlas of transport systems in brain regions at different time points during co-culture. Data normalization was performed using the samples obtained on the first day of the model. Blue represents downregulated gene expression, while red represents upregulated gene expression.

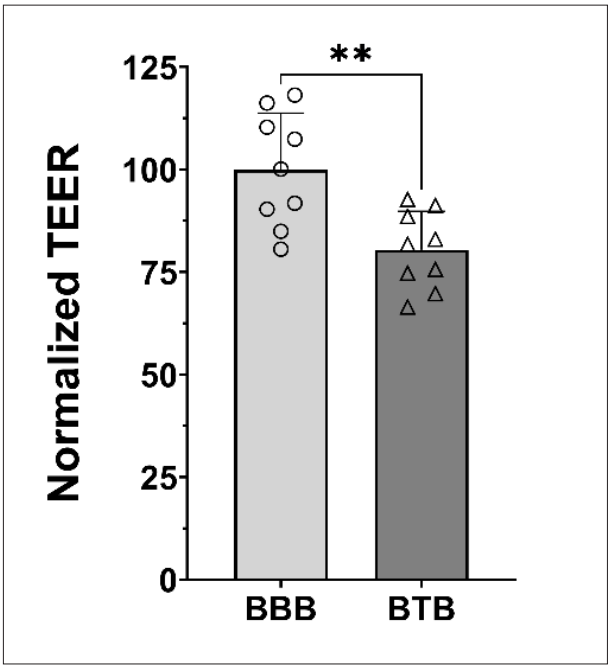

Figure S11. TEER values of the BBB and the BTB.

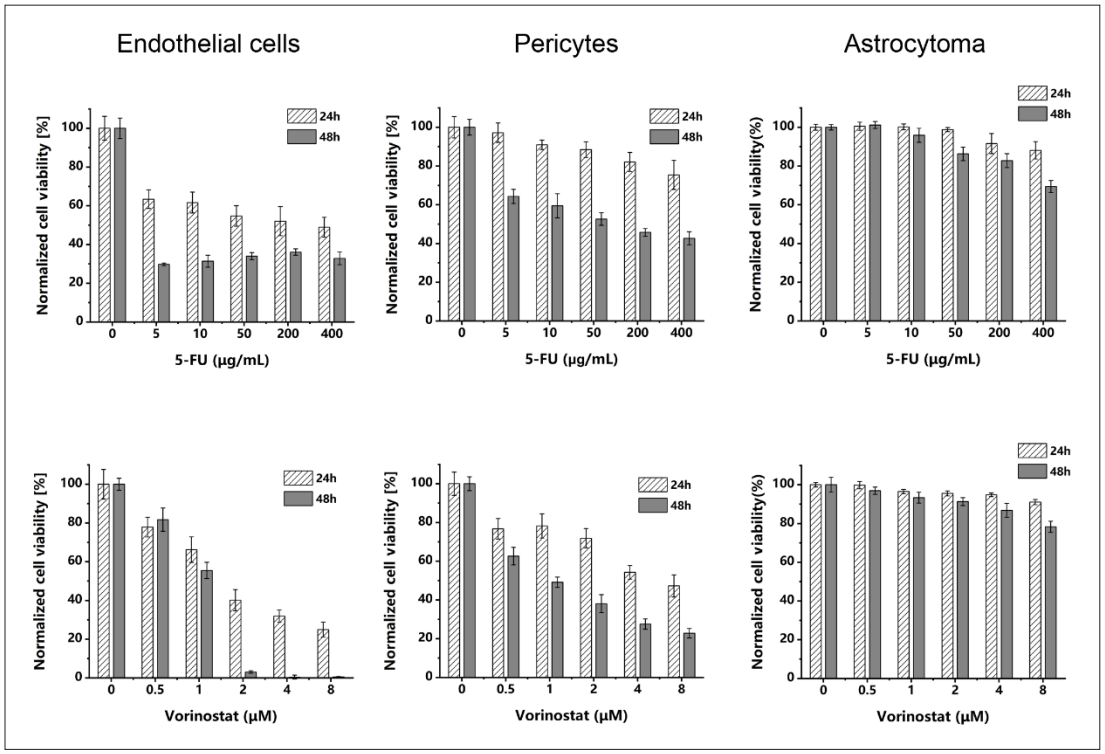

Figure S12. Drug cytotoxicity assessment of brain vascular constituent cells (ECs, pericytes, and astrocytoma). $n = 3$, independent experiments. Data are presented as the mean ± S.D. Significant differences between the groups were determined by *t*-test.

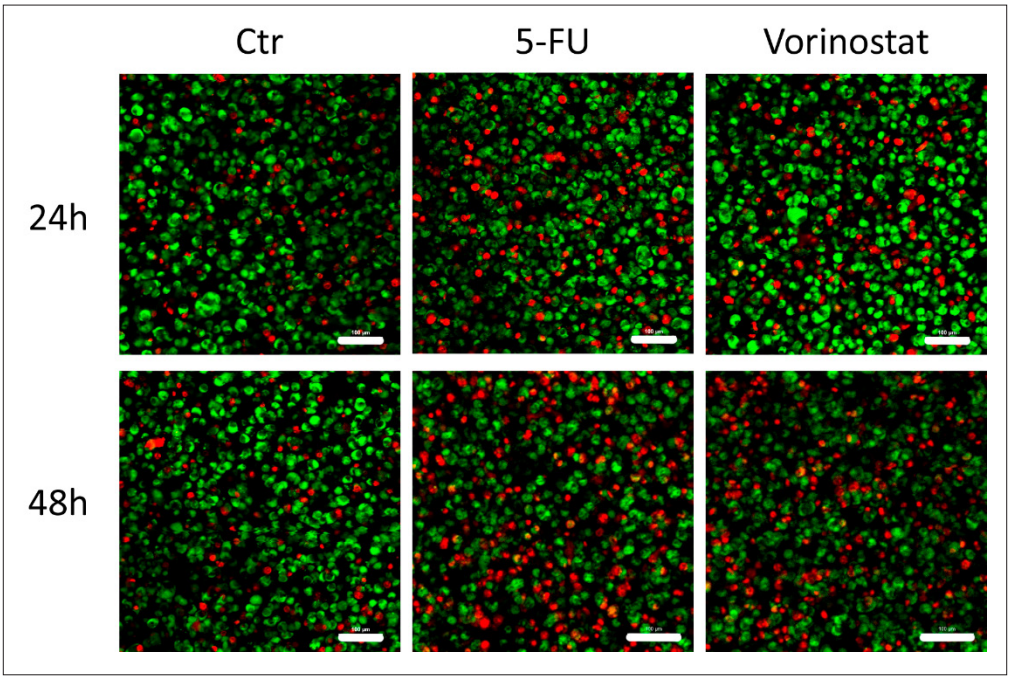

Figure S13. Live-dead imaging comparison of hNVU chip (with astrocytoma cells) under the action of chemotherapeutic drugs. 5-FU, 50 μg/mL; vorinostat, 0.9 μM. Scale bar: 100 μm.

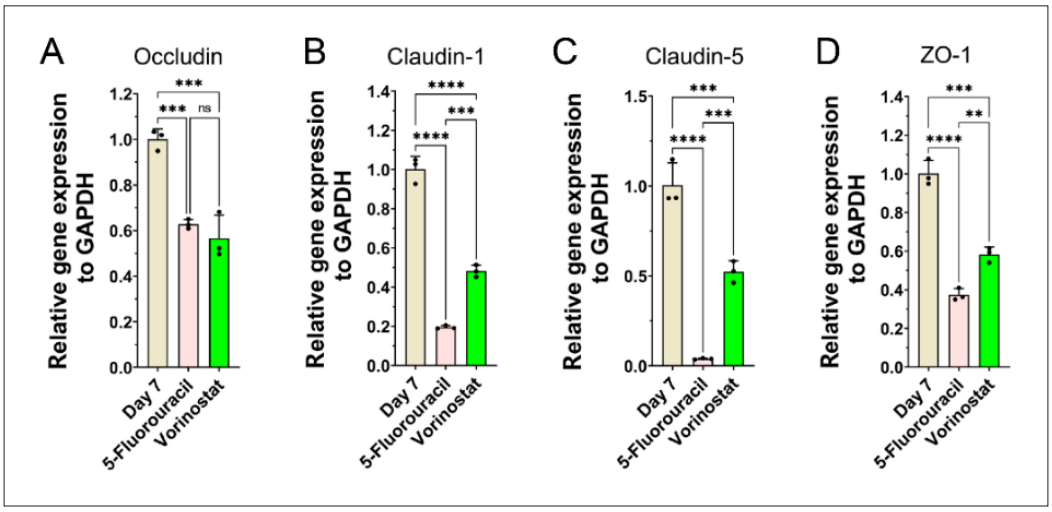

Figure S14. Gene expression of tight junctions.

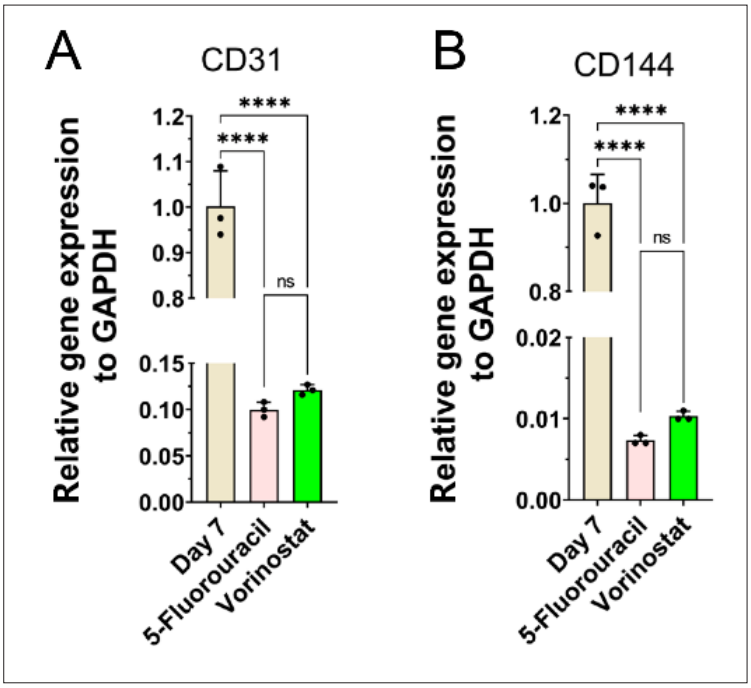

Figure S15. Gene expression of adhesion junctions.

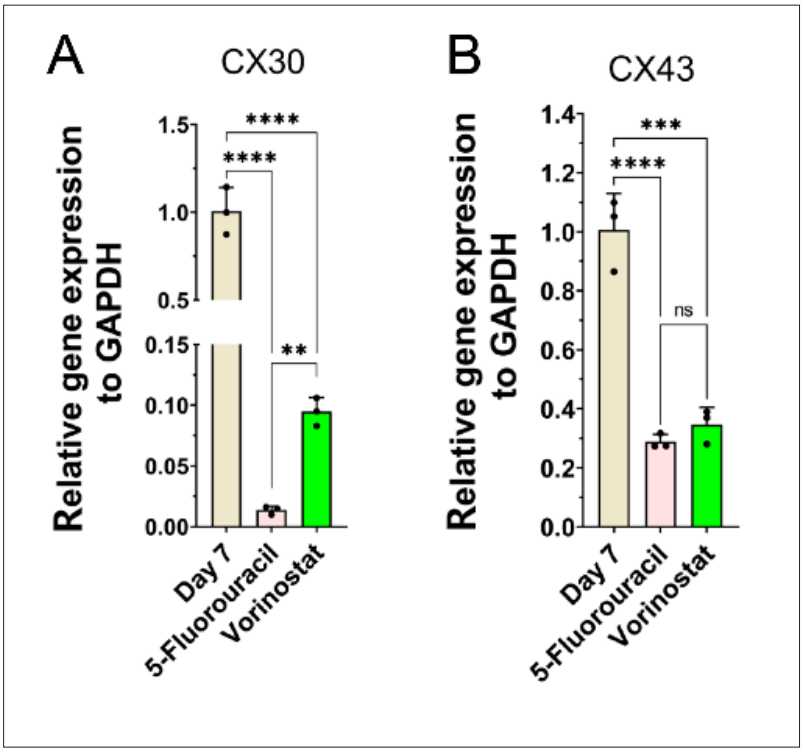

Figure S16. Gene expression of gap junctions.

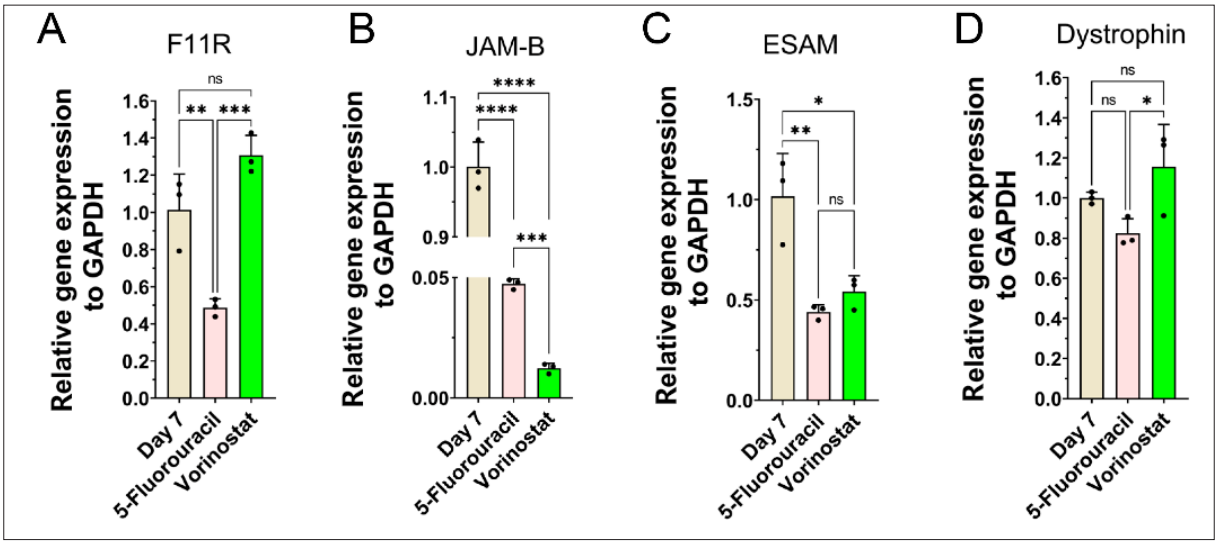

Figure S17. Gene expression of cytoskeletons and other molecules.

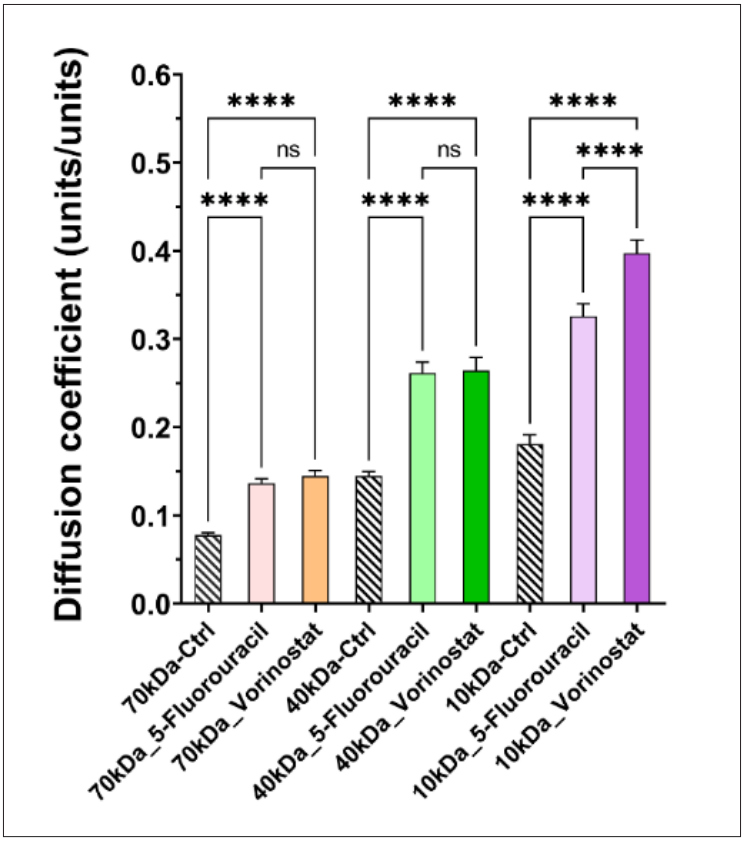

Figure S18. Permeability of the blood–brain barrier under the action of the drug.

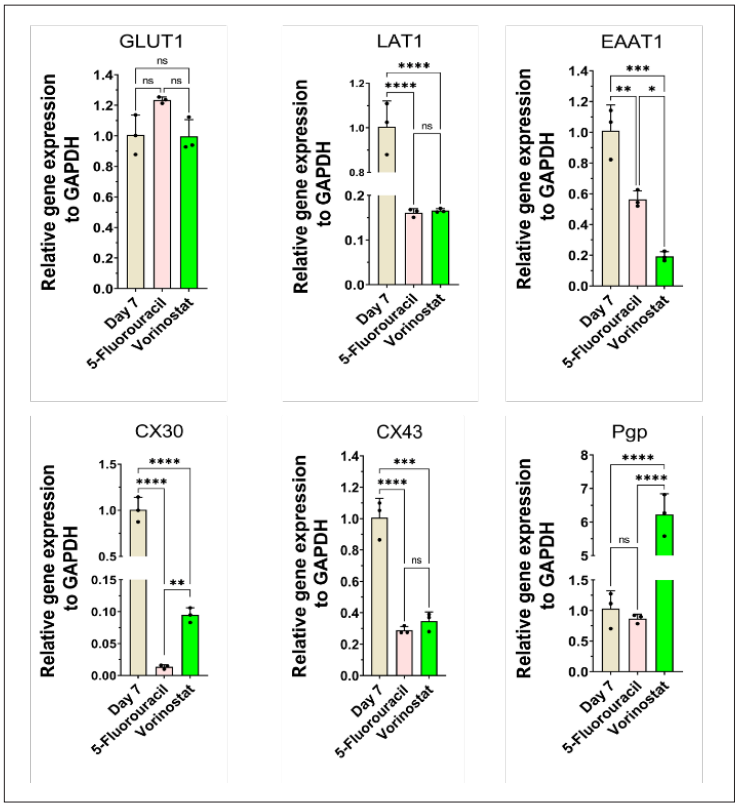

Figure S19. Chemotherapeutic drugs 5-fluorouracil and vorinostat interfere with metabolic functions and transporters in the BTB. n = 3, independent experiments. Data are presented as the mean ± S.D. Significant differences between the groups were determined by t-test.

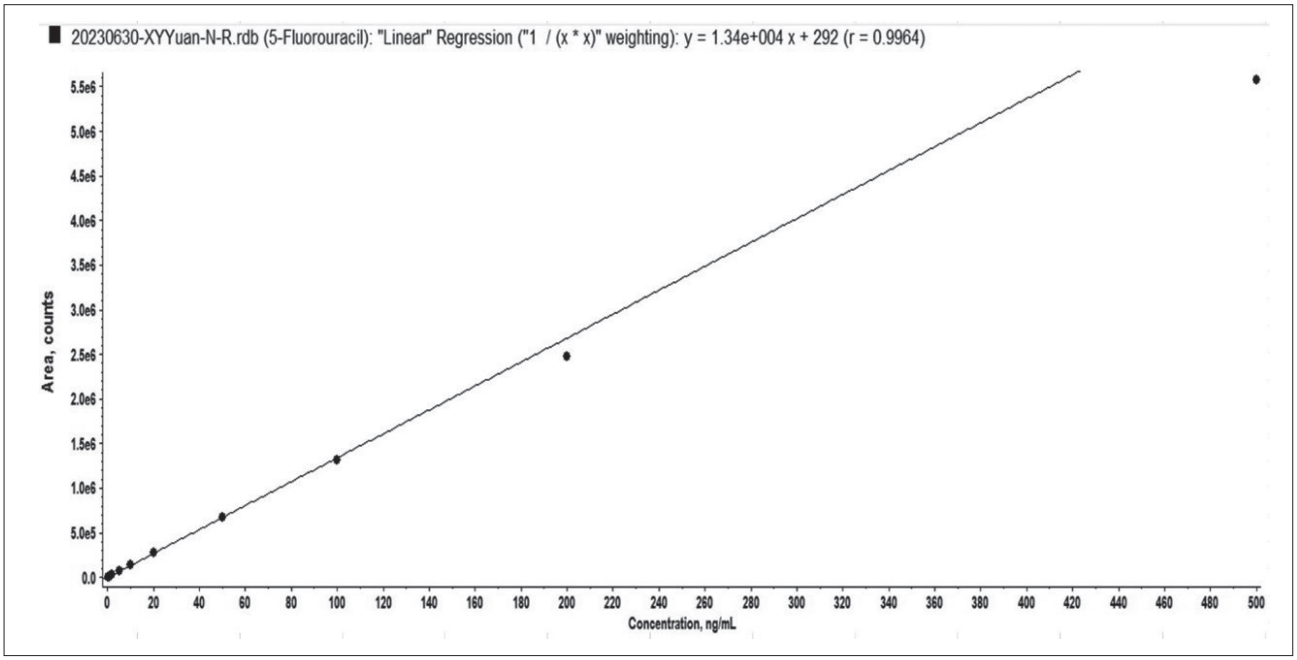

Figure S20. Standard curve of 5-fluorouracil concentration detected and analyzed by HPLC.

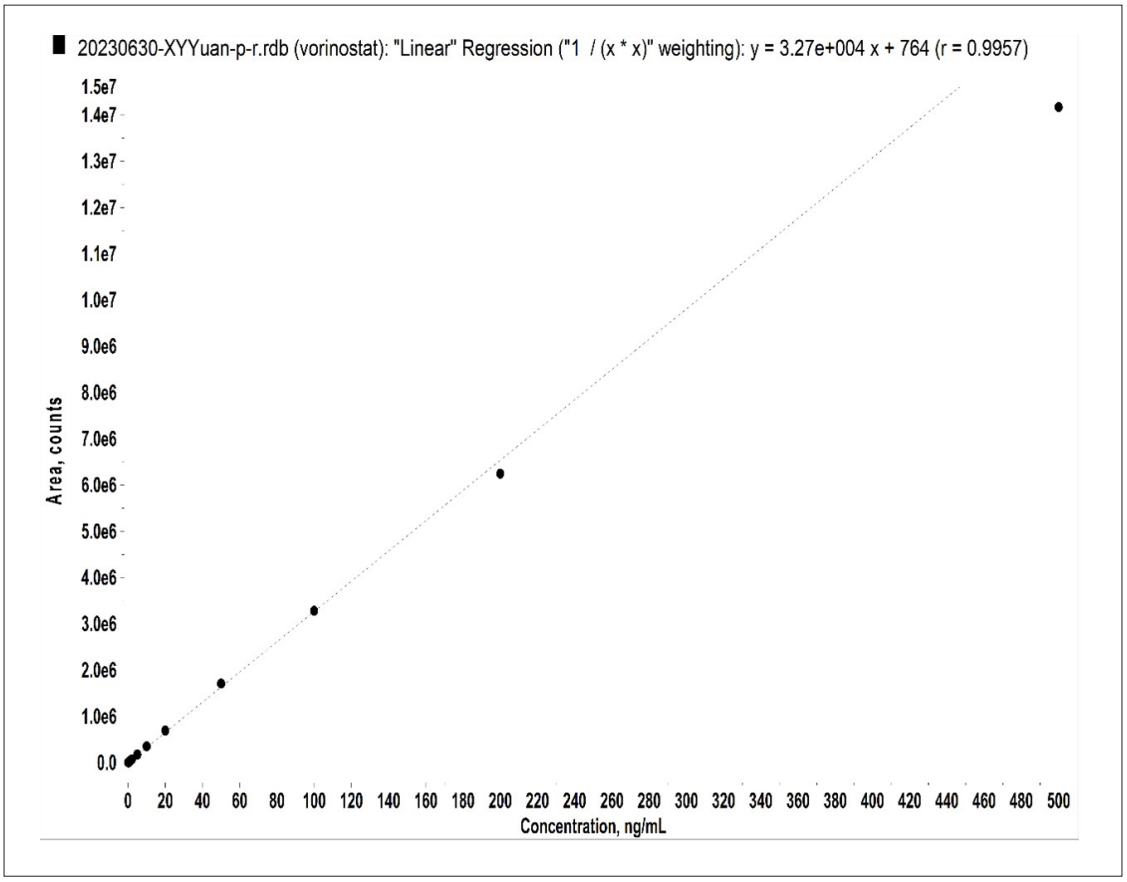

Figure S21. Standard curve of vorinostat concentration detected and analyzed by HPLC.

3. Supplementary tables

Table S1. Primer sequence for qRT-PCR

Target gene	Forward primer sequence (5'-3')	Reverse primer sequence (5'- 3')
CD31	GTCGGACAGTGGGACGTATATC	ACCTCAAACTGGGCATCATAAGA
CD144	CGACTACCAGGACGCTTTCA	AGGGCTCATGTATCGGAGGT
ZO-1	GAAGATTTGGCCGAGGGATAGAA	CCATCTCTTGCTGCCAAACTATC
Laminin	GTTTGGCGGATTCCTGAAATACA	AGGCACAAGTCTAACCACGTTTA
Collagen IV	GGGATGCTGTTGAAAGGTGAAAG	AACTTGAGCTTGTCCTGGTACTC
NG2	GGGTGGTTTCAGATCGGGAG	GCCAGGACTCTGAAGTGGTC
GFAP	GGCACGAGCAAAGTGAAGAC	AGGACCCTTCTTCGGCCTTA
Aquaporin 4	CAGGGGTCTATCGCCTTGTG	TCTCCTGGGAGCAGCACTATG
S100β	AGGAAATCAAAGAGCAGGAGGTT	TGGCTGCTTTCTAATCTCACTCA
IBA1	TGAGAAGACTGGTGGGAGAGAAG	GTTGATCTCATCCAGCCTCTCTT
CD14	AACACAGGAATGGAGACGCC	GCGAACGACAGATTGAGGGA
Tubulin	CTGGACCGCATCTCTGTGTACTA	GTACCACATCCAGGACAGAATCA
Nestin	CCGCTAAGGTGAAAAGGGGT	CCTTTTCCAGCTGACGGGAT
αSMA	CCTGACCCTGAAGTACCCGATAG	GGCAACACGAAGCTCATTGTAGA
SM22α	TCCAGACTGTTGACCTCTTTGAA	GCTCCTGCGCTTTCTTCATAAAC

(*Continued....*)

Table S1. (*Continued....*)

HDAC1	GCTCCACATCAGTCCTTCCAATA	ATTCGTTTGTCAGAGGAGCAGAT
TYMS	TTGGAGGAGTTGCTGTGGTTTAT	GGTCAACTCCCTGTCCTGAATAA
P53	ACCTATGGAAACTACTTCCTGAAAA	CTCTGGCATTCTGGGAGCTT
PTEN	CTCAGCCGTTACCTGTGTGT	AGGTTTCCTCTGGTCCTGGT
CDK4	GAGCATGTAGACCAGGACCTAAG	GTTCCACCACTTGTCACCAGAAT
DPYD	GGTGGAATTGACTCTGCTGAAAG	CTGTCCATCCCAGTCTTGTAGTT
GLUT1	TTCACTGTCGTGTCGCTGTT	GGCCACGATGCTCAGATAGG
LAT1	GGAAGGGTGATGTGTCCAATCTA	GCAAAGAGGCCGCTGTATAATG
P-GP	CGGTTTGGAGCCTACTTGGT	TTCCGTGCTGTAGCTGTCAA
EAAT1	TGCAAAGAAGAGACCCTCCTAGA	TTCTGTATGGTCGGAGGGTAAAT
Occludin	CCAATGTCGAGGAGTGGGTTAAA	AGTCATCCACAGGCGAAGTTAAT
Claudin-1	GAAGACGATGAGGTGCAGAAGAT	CCAAATTCGTACCTGGCATTGAC
Claudin-3	AGCAACATCATCACGTCGCAGAA	CAGTGCCAGCAGCGAGTCGTA
Claudin-5	CCTGCCCTTAACAGACGGAA	GCCTCTGGGAAGTAAGGCAG
Claudin-12	CGTTGGCAGTTGGCCTTAAC	AGGCTAGCACAGGTGCCTTA
ZO-2	TCACTGCAAACACACCTTGGA	GAGTGGGAACCTCGGTCCAT
ZO-3	CCTATGAACGGGAAGCCCTG	TCGAGAGGTCACAGGTCAGT
FN1	GAGGGCAGAAGAGACAACATGAA	CCCTTCATTGGTTGTGCAGATTT
JAM-A	ACCACCAGACTCGTTTGCTATAA	GCCTTCCTCAGAGACCATACAAG
JAM-B	CTGTGAAGCCCGCAATTCTG	CCACAACTACTACGGCTGCT
JAM-C	CTCGGCTGCCTGACTTCTT	GGGTCACTTGTCTGCGAATCC
ESAM	GAGTAAGCCCGCTGTCCAATAC	CGAAAGGTTGGTGAGGCTTAAAG
CX30	CTCCAGAAGGCAATACCAACC	GCTCCTTTGTCAAGCAGTCTC
CX43	AGGAGTTCAATCACTTGGCGT	CTCCAGCAGTTGAGTAGGCTT
Dystrophin	GGCCTCCTTCTGCATGATTCTAT	CCGCTTCGATCTCTGGCTTATTA
GAPDH	GGAGTCCACTGGCGTCTTCA	GTCATGAGTCCTTCCACGATACC
ABCG2	TCAGATGGGTTTCCAAGCGT	CACTGGTTGGTCGTCAGGAA
ABCC1	GCGATGAAGACCAAGACGTATCA	GACAGGTAGGCAGACTTCTTCAG
ABCC4	ACCTTCTCAGAGTCTTCGGTTTG	GCCACCAATCTTGAAGCACATAG
ABCC5	GTGTGGTCTCTGTCCAAGCA	TCATCAGGCACACGATGGAC
SLC5A1	GCCTTGCCCCAGAAAGACAAA	CCAACATCTCCCCAGTCCCTC
SLC2A13	GACTCAGAAGGCCCGTAGAATTT	GTAGGCCACAACCCACAATTAAA
SLC7A1	GGCTGAGGATGGACTGCTATTTA	GTATACCAGGTTAGGCTGCTCTG
SLC7A6	GAAACCTCTCTCTTGCCCTCTAC	ATGAGCGTCACAATTGGCATAGA
SLC38A1	TGGCAAACACTGGAATCCTACTT	ATACACCATGCAGCCTGTTTCTT
SLC38A3	GCTCAACTCACAGACAGCATACA	TAGAAGGTGAGGTAGCCGAAGAG
SLC1A4	TCCGTACGTATGCAACCGATTAT	TCCTTCGGAGCCTAGTTTCTTTAA
SLC6A9	ACGGCATCATGTACTACCTAACC	GAAGATGACGAAGCCAGCATAGA
SLC6A6	GGTGCGTTTCTCATACCGTATTT	AGACATTCAGGAGGGACACAATT
SLC16A1	TCTGTGTCTATGCGGGATTCTTT	ACATGTCATTGAGCCGACCTAAA
SLC16A7	TGAGGATTCAGTGCAGCTTTACT	GCTGTACCACGCTGCTACTAAAG
SLC16A2	TAAGAATCAGGCAGTCGCCC	TGGTGCATAAGAGGCTGCAT
SLC27A1	CGATATACCAGGAGCTGCAGAAG	AGCCTCGTCTTCTGGATCTTGAA
SLC28A2	TACCTGGTCCCAAACGTCAA	CCTGTATCCTTTTGAAACCCTTCC

(*Continued....*)

Table S1. (*Continued....*)

SLC29A2	TGCTTCCTCCTCTTCAACATCAT	GGACACCAGGTAGCCATTAGAAA
SLCO2B1	CAGGGCTTTGAGACTTTCCCA	AACCTGGGAAACAAGAGGGATG
SLCO1C1	TAGGATGGAGCAGAACATGGAG	ATAGTCACTTATAGCGCCACACAA
SLC22A1	ACCTTCCTCTTCCTGCTCTACTA	CGGAACAGGTCTGCAAATGAAG
SLC22A5	GCTCATCTCTCAGGGACGATTTG	TTGTAACTCACTCGGGTCAAAGA
SLC29A4	GATGAGCTTCACCTTCGACAGTC	GCAAAGTAGATGGCGTGATAACG
SLC44A1	GCTGGGATTATGCTGCTCAACTA	CCACAAACTCCATCAGCACTTTA
SLC5A6	GCCTGGTCATGTTCGCGTATTA	TTCCATCGTAACAGTTGCCAATG
AVPR1A	TTTCCTGGGGCAACTGAATGA	AAGACAACACACAGTAAAATTGAGG
TFRC	AGCCCACTGTTGTATACGCTTAT	AGGGAAAGCAGCATTGTCTAAAG
LRP1	AGATGAGTCCAATGCCACTTGTT	AGATGAGTCCAATGCCACTTGTT
AGER	TCAGCATCAGCATCATCGAACC	GCCGCCTTTGCCACAAGAT
MFSD2a	GCCTTGTTTCCAGGACCTCAATA	CTGGGCTTCATAGGGTTCTCTCT
FN1	GAGGGCAGAAGAGACAACATGAA	CCCTTCATTGGTTGTGCAGATTT
COL4A5	CTCTTGGTTTCCCTGGACAGAAA	ACTCTCCTTTGTCACCCTTCATT
LAMA5	TGGAAGTCCTCATCAACGCC	ATAATCCAGCCAGAGCCACC
SPARC	TGACAACAAGACCTTCGACTCTT	ATGTATTTGCAAGGCCCGATGTA
NID1	CTGTGACGAGCTACGGGAAG	GGGTTGGAAAGCATCCGTCT
AGRN	TCCGAAGCCAGAAATGCCTTA	TTAGTAACACGGCACCCAGC
FGB	AGCACTCTCCACTTAGCAACC	AGGACACTTGAACTCCCTGC

Table S2. Primary and secondary antibodies/probes for immunocytochemistry

Antibody/Probe	Species	Dilution ratio/concentration	Manufacturer and catalog number
CD31	Rabbit	1:100	Abcam #ab76533
CD144	Mouse	5 μg/mL	Thermo #14-1449-82
ZO-1	Rabbit	1:100	Abcam #ab96587
Laminin	Rabbit	1:100	Abcam #ab11575
Collagen IV	Mouse	1:100	Abcam #ab86042
NG2	Rabbit	1:250	Abcam #ab255811
GFAP	Rabbit	1:100	Abcam #ab278054
Aquaporin 4	Rabbit	1 μg/mL	Thermo #PA5-53234
S100β	Rabbit	1:100	Thermo #710363
IBA1	Rabbit	0.5 μg/mL	Abcam #ab178846
β3-Tubulin	Mouse	1 μg/mL	Abcam #ab78078
Anti-rabbit Alexa Fluor 488	Goat	1:200	Thermo Fisher Scientific #A11008
Anti-rabbit Alexa Fluor 594	Goat	1:200	Thermo Fisher Scientific #A11037
Anti-mouse Alexa Fluor 488	Goat	1:200	Thermo Fisher Scientific #A11029
Anti-mouse Alexa Fluor 594	Goat	1:200	Thermo Fisher Scientific #A11005